Diagnosing New York City's Noises with Ubiquitous Data

Yu Zheng[1], **Tong Liu**[1,2], **Yilun Wang**[1], **Yanmin Zhu**[2], **Yanchi Liu**[3], **Eric Chang**[1]
[1]Microsoft Research, Beijing, China
[2]Shanghai Jiao Tong University, Shanghai, China
[3]Information Systems Department, New Jersey Institute of Technology, Newark, NJ, United States
{yuzheng, v-tongli, v-yilwan, echang}@microsoft.com; yzhu@cs.sjtu.edu.cn; yanchilyc@gmail.com

ABSTRACT
Many cities suffer from noise pollution, which compromises people's working efficiency and even mental health. New York City (NYC) has opened a platform, entitled 311, to allow people to complain about the city's issues by using a mobile app or making a phone call; *noise* is the third largest category of complaints in the 311 data. As each complaint about noises is associated with a location, a time stamp, and a fine-grained noise category, such as "*Loud Music"* or "*Construction"*, the data is actually a result of "*human as a sensor*" and "*crowd sensing*", containing rich human intelligence that can help diagnose urban noises. In this paper we infer the fine-grained noise situation (consisting of a noise pollution indicator and the composition of noises) of different times of day for each region of NYC, by using the 311 complaint data together with social media, road network data, and Points of Interests (POIs). We model the noise situation of NYC with a three dimension tensor, where the three dimensions stand for regions, noise categories, and time slots, respectively. Supplementing the missing entries of the tensor through a context-aware tensor decomposition approach, we recover the noise situation throughout NYC. The information can inform people and officials' decision making. We evaluate our method with four real datasets, verifying the advantages of our method beyond four baselines, such as the interpolation-based approach.

Author Keywords
Urban computing; urban noises; social media; big data

ACM Classification Keywords
H.2.8 [**Database Management**]: Database Applications - *data mining, Spatial databases and GIS*;

General Terms
Algorithms, Experimentation.

INTRODUCTION
The rapid progress of urbanization modernizes people's lives, but also creates noise pollution in cities. In addition to compromising working efficiency and quality of sleep, urban noises may impair people's physical and mental health. People living in major cities, especially in NYC, are increasingly concerned about tackling the problem, calling for technology that can diagnose the citywide noise situation and the composition of noises in different places.

Modeling citywide noises, however, is very difficult, as the level of noises varies by locations and changes over time significantly. Moreover, besides the level of sound measured in decibels, the measurement of noise pollution also depends on people's tolerance to noises, which changes over different times of day. For example, at night, people's tolerance to noises is much lower than during the daytime. A quieter noise at night may be considered a heavier noise pollution. Consequently, even if we could deploy sound sensors everywhere, diagnosing urban noise pollution solely based on sensor data is not thorough. Furthermore, urban noises are usually a mixture of multiple sound sources. Understanding the composition of noises, e.g., *in evening rush hour, 40 percent of noise in a given place comes from loud music, 30% from vehicle traffic and 10% from constructions*, is vital to tackling noise pollution.

While modeling urban noise pollution is very difficult, other ubiquitous data sources indicating urban noises are already available. For example, since 2010, NYC has operated a platform that allows people to call 311 to complain about what they feel annoyed by (without being an emergency) in the city [1]. According to 311 records from 2010 to 2014, the third largest category of complaints has been about urban noises. When complaining about noises, people are required to provide the location, time and a fine-grained noise category, such as loud music or construction. This means that the 311 complaint data about noises is actually a result of "*human as a sensor*" and "*crowd sensing*", containing rich human intelligence that can help us understand noise pollution from people's perspectives. Specifically, the number of 311 calls (about noises) made in a location is an indicator of the noise pollution of the location (see Figure 5), and the distribution of these 311 complaints over different noise categories may describe the composition of noises in the location. On the other hand, the 311 data is very sparse (see Figure 6 for details), as there are not always people reporting ambient noises at a given place and time. Recovering the noise situation of locations that do not have sufficient 311 data remains a challenge.

Fortunately, the big data era has brought us unprecedented data in urban areas, such as user check-in data from location-based social networks, POIs, and road networks. Those data

Ubicomp '14, September 13 - 17 2014, Seattle, WA, USA

sources also have a correlation with urban noises, providing complementary information to pinpointing urban noises. For instance, a region with a denser road network is more likely to embrace heavier traffic noises. Likewise, a region with many bars is very likely to generate music noises in the evening. Additionally, a bar with more user check-ins would generate a louder noise (see later sections for more details).

In this paper, we infer the noise situation (consisting of a noise pollution indicator and a noise composition) of arbitrary regions of NYC, at different time intervals of a day, by combining the historical 311 noise complaint data over a period of time with social media, POIs, and road network data. According to the noise pollution indicator, we can rank locations in different time spans, e.g. 0am-5am on weekdays and 7pm-11pm on weekends, as illustrated in Figure 1 A); the darker the color is the heavier the noise pollution is. Or, we can rank locations by a particular noise category, such as construction, as depicted in Figure 1 B). We can also check the noise composition of a particular location changing over time, e.g. Time Square, as shown in Figure 1 C).

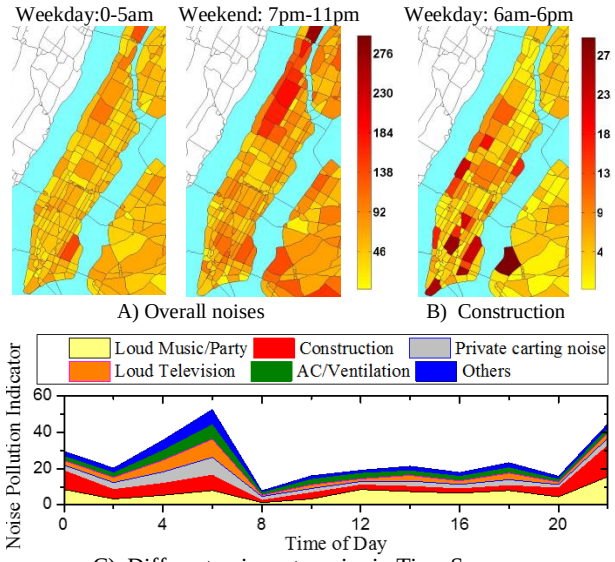

A) Overall noises B) Construction

C) Different noise categories in Time Square

Figure 1. Results of our research

To achieve these goals, we first partition NYC into disjoint regions by major roads, using a map segmentation algorithm [24]. We then map the 311 noise complaints onto these regions according to their geospatial locations, building a three dimension tensor, where the three dimensions denote regions, categories of noises and time slots. Each entry of the tensor stores the number of 311 complaints about a particular noise category in a particular region and a particular time slot. We fill in the tensor's missing entries (i.e., without 311 complaints), using a context-aware tensor decomposition approach that combines 311 data with user check-ins, road network data and POIs. After that, the value of an entry is used as a noise pollution indicator of a region in a time slot and in a noise category, and the values of the entries across different categories denote the composition of noises in the region. Our approach has three primary contributions:

- *Citywide noise modeling*: Beyond raw sensor data, the 311 data indicates not only the level of noise in a place but also people's reaction and tolerance to different categories of noise and during different time spans of a day. Using a 3D tensor, we simultaneously model the correlation of noises among different locations, time spans and noise categories.
- *Dealing with data sparsity*: The 311 data is very sparse, resulting in a sparse tensor. Filling in the missing entries of the tensor solely based on non-zero entries is not accurate enough. To deal with the data sparsity of the tensor, we extract three categories of features from users' check-in data, POIs and road network data. From different perspectives and built from other data sources, the three feature sets represent the temporal correlation between different time slots, the geospatial correlation between different regions, and the correlation between different noise categories. By feeding these feature sets into the tensor decomposition process, we reduce the error of tensor decomposition, thereby improving the accuracy of noise inferences.
- *Real evaluation*: We evaluated our method by extensive experiments that use four real data sets [31]. The results demonstrate the advantages of our method beyond four baselines, such as Kriging [14], and reveal interesting discoveries that can bring social good to NYC.

The rest of this paper is organized as follows: the second section overviews the framework of our method. The third section describes the datasets we use and how they are correlated with noises. The fourth section introduces the method for noise inferences, and the fifth section presents results and visualizations. The sixth section summarizes the related work, followed by the conclusion in the last section.

OVERVIEW

Preliminary

Definition 1 (*Road Network*): A road network RN is comprised of a set of road segments $\{s\}$ connected between each other in the format of a graph. Each road segment s has two terminal nodes, a series of intermediate points between the two terminals, a length $s.len$, a classification (level) $s.lev$ (e.g., a highway or a street). The smaller $s.lev$ of road segment s is, the higher the level of s is.

Definition 2 (*POI*): A point of interest (POI) is a venue in a physical world, like a shopping mall or theatre, having a name, address, coordinates, category, and other attributes.

Definition 3 (*User Check-in*): In a location-based social networking service (e.g., Foursquare), a user can mark a venue (e.g. a shopping mall) when the user arrives there, which is known as a check-in. Each check-in has a time stamp and a geospatial coordinate, usually associated with a POI category, such as food and dining.

Definition 4 (*Noise Complaint*): Each noise complaint ns contains a timestamp, a location $ns.l$ denoted by a (latitude, longitude) or street address, and a complaint category $ns.c$.

Framework

Figure 2 presents the architecture of our system, which consists of three major layers: 1) data acquisition, 2) noise inference, and 3) service providing. We will detail the first two layers in the following sections respectively.

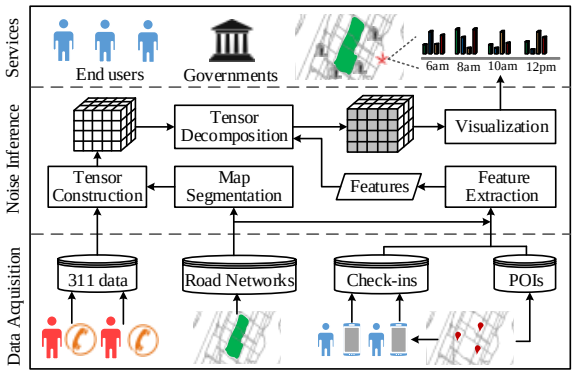

Figure 2. The architecture of our method

DATA ACQUISITION AND ANALYSIS

This section introduces four data sources, and analyzes the correlation between them and NYC's noises.

311 Data about Noises

311 is NYC's governmental non-emergency service number, allowing people in the city to complain about everything that is not urgent by making a phone call, or texting, or using a mobile app. According to the 311 data recorded from May 23, 2013 to Jan. 31, 2014 (168 weekdays and 68 weekends), 67,378 complaints were about urban noise, which is ranked the third largest out of the 187 complaint categories. Table 1 shows the 14 fine-grained noise categories and their proportions in the total number of noise complaints. *Loud music/party* is the largest. Figure 3 paints the 236-day 311 complaints about noises on a digital map, where the height of a bar denotes the number of complaints in a location. For example, we can see that south Manhattan was suffering from *Construction* and *Loud music/party*.

Table 1. Categories of noise and their proportion in 311 data

Categories	%	Categories	%
c_1. Loud Music/Party	42.2	c_8. Alarms	1.7
c_2. Construction	17.2	c_9. Private carting noise	0.8
c_3. Loud Talking	14.6	c_{10}. Manufacturing	0.3
c_4. Vehicle	13.7	c_{11}. Lawn care equipment	0.3
c_5. AC/Ventilation	3.9	c_{12}. Horn Honking	0.2
c_6.Banging/Pounding	2.1	c_{13}. Loud Television	0.1
c_7. Jack Hammering	2.1	c_{14}. Others	0.8

Figure 4 shows the number of 311 complaints in the top five noise categories changing over time of day, where the complaints of the 68 weekend days are aggregated into one day. As the number of weekdays (168) is more than weekend days, we randomly select 68 weekdays and aggregate the complaints of these days into one day, for a fair comparison with weekend days. It is interesting that more complaints were made at night than daytime. This indicates that people's tolerance for noise is lower at night. Generally, weekends have much more noise complaints than workdays. This could be for two possible reasons. One is weekends could have more sources of noises than weekdays, such as football games and parties. The other is people have more time to complain during the weekends. Staying at home, their expectation for a quiet day is higher than a workday. Specifically, weekends have less complaints about air conditions/ventilation than weekdays. The reason is very intuitive. The air conditioning and ventilation systems of many buildings may be suspended during weekends.

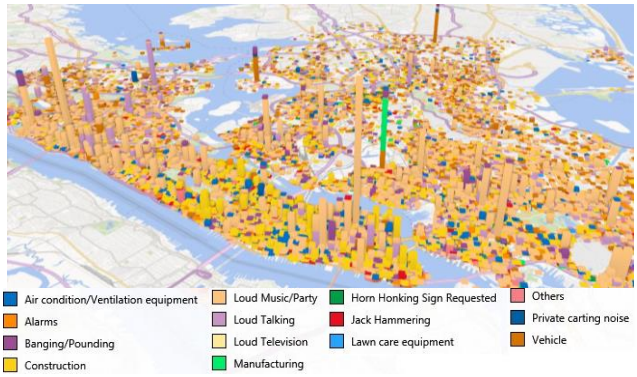

Figure 3. Complaints of noises in NYC (5/23/2013 to 1/13/2014)

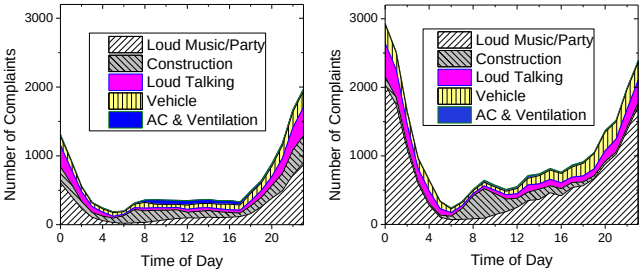

A) Weekdays B) Weekends

Figure 4. Number of complaints changing over time of day

The data presented in Figure 3 and 4 well demonstrates the value of "*human as a sensor*" and "*crowd sensing*", where each individual contributes their own information about the ambient noises; the individual information is then aggregated to diagnose the noise pollution throughout a city. The noise categories tagged by a complainer can help analyze the composition of noises in a location. We also find 311 noise complaints in a location have a correlation with its real noise level. Figure 5 studies the number of noise complaints and real noise levels (collected through a mobile phone) in 36 locations, in daytime and nighttime respectively. [12] details how we collect real noise levels. First, given *the same time span* in a day, the more 311 calls are made in a location, the louder the real noise is in the location. We see the same trend in Figure 5 B) and C). If given sufficient 311 complaints of any location and at anytime, we can recover the noise situation throughout the city by doing some simple statistical analysis on the complaint data. On the other hand, there are some locations (marked by the red circles shown in Figure 5) having very few 311 complaints but still with considerable real noises. This is caused by the sparsity of 311 complaint data, i.e., having no complaint records does not mean no noise. To diagnose the noises throughout a city, we need to recover these *missing* locations. Second, the data of different

time spans are not comparable. As shown in Figure 5 C), the real noise level at 6am-6pm is actually higher than 7pm-11pm; however, more complaints were made in the latter time span, as people's tolerance to noises is much lower at night. The discovery reveals the advantage of 311 data beyond raw sound data. This also motivates us to model the noise situation in different time spans respectively.

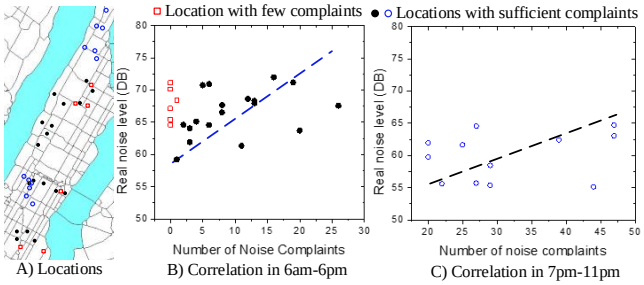

Figure 5. Correlation between 311 complaints and real noise level: A) shows the geo-distribution of the 36 locations in NYC that we test, B) plots the correlation during the time span 6am-6pm. The blue broken line fits the majority of points except for those falling in the red circle.

Figures 6 and 7 further explore the sparsity of the 311 data. Each plot in Figure 6 denotes the proportion of regions (see Definition 5) with the number of complaints smaller than its value on the horizontal axis. For instance, over 90 percent of regions have received less than 60 complaints in total in the 68 weekdays (i.e. less than one complaint per region per day). Figure 7 presents the proportion of regions having at least one complaint from the top five most frequent noise categories. While a few regions may not really have any noise pollution, the majority of regions without 311 data are due to lack of people reporting noise. Given the sparseness of the complaints, recovering the noise situation throughout a city solely based on the complaint data is not good enough, so, we turn to other data sources for help.

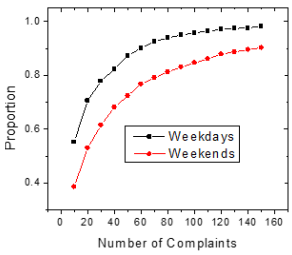

Figure 6. Proportion of regions with complaints smaller than a number

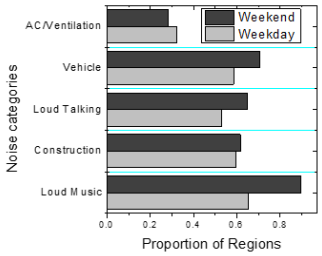

Figure 7. The proportion of regions with complaints of a noise category

User Check-in Data

User check-in data from location-based social networks denotes human mobility in cities, which is relevant to urban noise. First, people themselves are source of noise, talking loudly or playing music intensely. Second, human mobility indicates the traffic volume and function of a region [25][26]. These factors have a strong correlation with noises. To deal with the data sparsity problem of 311 data, we also collect from Gowalla 127,558 check-ins that were generated from 4/24/2009 to 10/13/2013 in NYC, and 173,275 check-ins from Foursquare (generated from 5/5/2008 to 7/23/2011) also in NYC. The check-in data from Foursquare are also associated with one or more categories: *Art & Entertainment*, *College & University*, *Food*, *Great Outdoors*, *Nightlife Spot*, *Home/work/other*, *Shop*, and *Travel spot*. As NYC has not changed tremendously recently, people's check-ins patterns have remained similar over the past two years. This allows us to correlate the check-in data of different times with the 311 data. Other types of human mobility data, such as mobile phone data or GPS traces of taxis, can also be applied here.

As shown in Figure 8 A), we found a strong correlation (Pearson correlation 0.873, P-value of T-Test << 0.001) between the number of check-ins in the *Art & Entertainment* category and the number of noise complaints about *vehicles* in each hour of a day. The number of check-ins and complaints are normalized into a value falling in [0, 1]. Likewise, the number of user check-ins at the *nightlife spot* category also has a positive correlation with the number of complaints in the category *Loud music/Party* (Pearson correlation 0.745, P-value of T-Test << 0.001). Figure 8 B) respectively presents the geospatial distributions of user check-ins (in *Art & Entertainment* and *Nightlife spot* categories) and the noise complaints (in *Loud music/party* category), where they have a similar geospatial distribution in some regions (marked by the dotted circles).

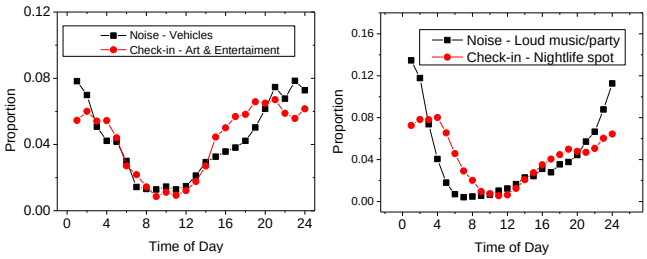

A) Temporal review: categories of check-ins vs categories of noises

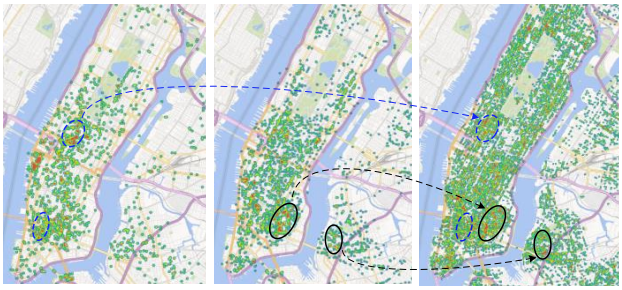

B) Geospatial distributions of check-ins and noise complaints

Figure 8. Correlation between user check-ins and 311 in NYC

Road Network and POIs

The information on POIs in a region, such as the number of POIs in different categories and the density of POIs, indicates the function of the region as well as the flow of people in the region, which are very relevant to a region's noise situation. For example, if a region has many bars, the amount of loud music and talking tend to be high. A park, however, is usually quiet. The structure of a road network in a region, like the number of intersections and the total length of road segments, also has a strong correlation with the region's traffic patterns, which is a major noise source.

Figure 9 shows the correlation between noise complaints in the *vehicles* category and a few road network/POI features (e.g. the total length of road segments, the number of intersections, and the density of POIs). Each column and row represents one feature; each marker is a region; different symbols stand for different numbers of complaints in the *vehicles* category, e.g. a green square denotes 1-5 complaints. So, each box in Figure 9 shows the 311 complaints in the *vehicles* category with respect to two road network/POI features. As illustrated in the box of the first row and second column, where its horizontal axis denotes the number of intersections in a region and the vertical axis means the total length of road segments in a region, we can clearly see that the more intersections a region has the more red crosses and purple triangles occur (denoting more complaints about *vehicles*). We also find a similar trend with respect to length of roads.

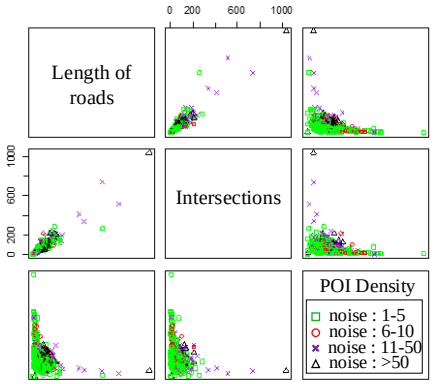

Figure 9. Correlation between the features of road network/POIs and the noises of vehicles

As illustrated in Figure 10 A) and B), the geospatial distribution of *Loud talking* noise complaints shares some similar regions (marked by the dotted circles) with the distribution of POIs of food. We also find the similarity between the distributions of noises of *Loud music* and the POIs of *Art & Entertainment*. So, POIs and road network data can be treated as complementary information, helping supplement the noises of regions without sufficient 311 data. There are still some differences between these distributions, as each piece of data may only tell us a part of the panoramic view of urban noises. That is the reason why we need to embrace multiple data sources.

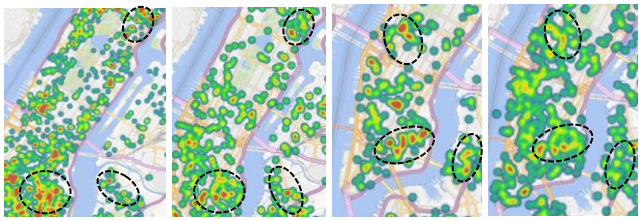

A) Loud talking B) POI: Food C) Loud Music D) POI: Entertainment

Figure 10. Geospatial distributions of POIs and noise complaints

NOISE INFERENCE

Map Segmentation

We partition NYC's map into disjoint regions, $\boldsymbol{r} = [r_1, r_2, \cdots, r_i, \cdots, r_n]$, by major roads (with $s.lev$ <5), using a map segmentation algorithm we propose in [24]. A region bound by major roads may stand for a block or a community, carrying more semantic meanings than using uniform grid-based partition. We want to study the noise of a location as fine-grained as possible. But, this will lead to an even worse data sparsity problem, significantly reducing the accuracy of recovered noises. The map segmentation can also be done by using NYC ZIP codes. We find that the regions segmented by the road network are finer than by ZIP codes.

The algorithm chooses the raster-based model to represent the road network and utilize morphological image processing techniques to segment a map. Specifically, a raster-based map is regarded as a binary image (e.g., 0 stands for road segments and 1 stands for blank space). In order to remove the unnecessary details, such as the lanes of a road and overpasses, the algorithm first performs a dilation operation to thicken the roads, as demonstrated in Figure 11 B). Second, the algorithm obtains the skeleton of the road networks by performing a thinning operation. This operation recovers the size of a region which was reduced by the dilation operation, while keeping the connectivity between regions. Finally, by clustering "1"-labeled grids through a connected component labeling (CCL) algorithm, individual regions can be found.

A) Raster-based map B) Dilation operation C) Thinning operation

Figure 11. Map Segmentation by major roads

Definition 5. *(Region):* Each region may consist of a number of road segments and lands, standing for some connected neighborhoods or a community. We use regions as the minimal units to study urban noises, assuming each region could have a similar noise constitution while different regions could have different ones.

Tensor Construction

As shown in the left part of Figure 12, we model the noises in each region using a tensor, $\mathcal{A} \in \mathbb{R}^{N \times M \times L}$ with three dimensions denoting N regions, M noise categories, and L time slots, respectively. As weekdays and weekends have different noise patterns, we build a tensor for them separately:

- *Region dimension*: The first dimension denotes regions $\boldsymbol{r} = [r_1, r_2, \cdots, r_i, \cdots, r_N]$ obtained after the segmentation;
- *Time span dimension*: We divide a day into equal slots $\boldsymbol{t} = [t_1, t_2, \cdots, t_k, \cdots, t_L]$. Each time slot lasts for a period of time, e.g. 2pm-3pm. We project the 311 data over a long period of time into one day. As a result, the number of slots in the time dimension is fixed.
- *Category dimension*: This dimension denotes the categories shown in Table 1, $\boldsymbol{c} = [c_1, c_2, \cdots, c_j, \cdots c_M]$.

- *An entry*: An entry $\mathcal{A}(i,j,k)$ stores the total number of 311 complaints of category c_j in region r_i and time slot t_k over the given period of time (e.g., 68 weekends). For the entries with a value smaller than a threshold, e.g. 2, we regard them as a missing entry (i.e., filled with an inferred value). The value of each entry in tensor $\mathcal{A}$ is then normalized to [0, 1] for decomposition.

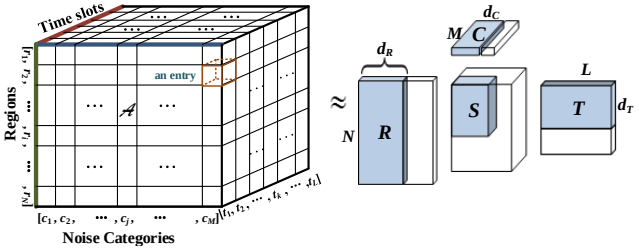

Figure 12. Structure of the noise tensor

A common approach to filling the missing entries of tensor $\mathcal{A}$ is to decompose $\mathcal{A}$ into the multiplication of a few (low-rank) matrices and a core tensor (or just a few vectors), based on $\mathcal{A}$'s non-zero entries. For example, as illustrated in the right part of Figure 12, we can decompose $\mathcal{A}$ into the multiplication of a core tensor $S \in \mathbb{R}^{d_R \times d_C \times d_T}$ and three matrices, $R \in \mathbb{R}^{N \times d_R}$, $C \in \mathbb{R}^{M \times d_C}$, $T \in \mathbb{R}^{L \times d_T}$, using a tucker decomposition model [7]. The objective function to control the error of the decomposition is usually defined as:

$$\mathcal{L}(S,R,C,T) = \frac{1}{2}\|\mathcal{A} - S \times_R R \times_C C \times_T T\|^2 + \frac{\lambda}{2}(\|S\|^2 + \|R\|^2 + \|C\|^2 + \|T\|^2), \quad (1)$$

where $\|\cdot\|^2$ denotes the l_2 norm; the first part is to control the decomposition error and $\frac{\lambda}{2}(\|S\|^2 + \|R\|^2 + \|U\|^2 + \|T\|^2)$ is a regularization penalty to avoid over-fitting; d_R, d_C, and d_T are usually very small, denoting the number of latent factors. λ is a parameter controlling the contribution of the regularization penalty. By minimizing the objective function, we can get optimized R, C, and T. Afterwards, we can recover the missing values in $\mathcal{A}$ by Equation 2:

$$\mathcal{A}_{rec} = S \times_R R \times_C C \times_T T. \quad (2)$$

The Symbol "$\times$" denotes the matrix multiplication; $\times_R$ stands for the tensor-matrix multiplication, where the subscript R stands for the mode of a tensor, e.g., $H = S \times_R R$ is $H_{ijk} = \sum_{i=1}^{d_R} S_{ijk} \times R_{ij}$;

Each entry's value in $\mathcal{A}_{rec}$ denotes the noise pollution indicator of a region in a time slot and a category. Given $\mathcal{A}_{rec}$, we can easily obtain the distribution of noise over different categories in region r_i, in a time slot t_k, by retrieving the vector $\mathcal{A}_{rec}(i,j,k), j = 1,2,\dots,M$. Or, we can rank regions in a time slot k by a noise category j, by using $\mathcal{A}_{rec}(i,j,k), i = 1,2,\dots,N$. Or, ranking regions according to overall noises by $\sum_j \sum_k \mathcal{A}_{rec}(i,j,k)$.

In our problem, however, the tensor is over sparse. For example, if setting 1 hour as a time slot, only 5.18% entries of $\mathcal{A}$ have values on weekends. Decomposing $\mathcal{A}$ solely based on its own non-zero entries is not accurate enough (we prove this in the experiments). So, we need to seek help from additional information sources.

Feature Extraction

To deal with the data sparsity problem, we extract three categories of features, geographical features, human mobility features and noise category correlation features (denoted by matrices X, Y, and Z), from POI/road network data, user check-ins, and 311 data, respectively. These features will be used as contexts in the decomposition process to reduce inference errors.

The geographical feature set is comprised of two parts: POI features $\boldsymbol{F_p}$ and road network features $\boldsymbol{F_r}$. As illustrated in Figure 13, road network features $\boldsymbol{F_r}$ consist of the number of intersections f_s (denoted as blue points) and the total length of road segments in different levels, f_r (e.g., $s.lev \in [1,6]$, $|f_r|$=6). The major roads binding a region are also counted in f_r. $\boldsymbol{F_p}$ is extracted from POIs falling in a region, consisting of the total number of POIs f_n, density of POIs f_d, and the distribution of POIs f_c over 15 categories: *Entertainment & Arts*, *Vehicles*, *Business to Business*, *Computers*, *Education*, *Food & Dining*, *Government*, *Health & Beauty*, *Home & Family*, *Legal & Finance*, *Professional & Services*, *Estate & Construction*, *Shopping*, *Sports & Recreation*, and *Travel*. By putting together the geographical features of a region into a vector, we formulate a matrix $X \in \mathbb{R}^{N \times P}$ (P denotes the dimension of geographical features), as illustrated in the bottom left part of Figure 13. Matrix X incorporates the similarity between two regions in terms of their geographic features. Intuitively, regions with similar geographic features could have a similar noise situation.

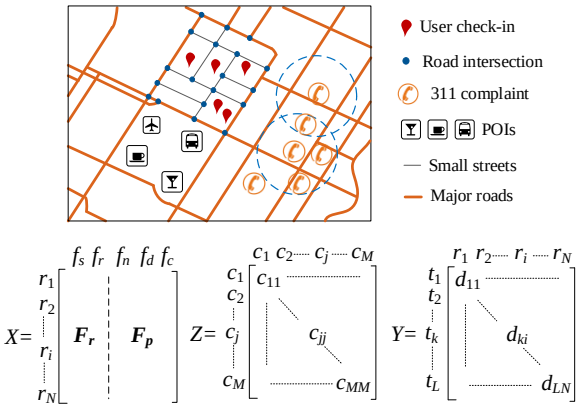

Figure 13. Feature extraction and representation

Human mobility features are derived from check-ins created by users in different regions and time slots. An entry d_{ki} of matrix $Y \in \mathbb{R}^{L \times N}$, shown in the bottom right part of Figure 13, denotes the number of check-ins generated in region r_i and time slot t_k. Matrix Y reveals the correlation between different time slots in terms of the distribution of check-ins over different regions. Two time slots sharing a similar user check-in pattern could have a similar noise situation.

The correlation between different noise categories can be learned from the 311 data itself. Once the correlation is determined, we can infer the presence of other categories in

a region given the observed category in the region. For example, *private carting noise* (c_9) has a strong correlation with *Jack Hammering* (c_7) on weekdays, as shown in Figure 14 A), while is correlated with *loud television* (c_{13}) on weekends, as illustrated in Figure 14 B). (Refer to Table 1)

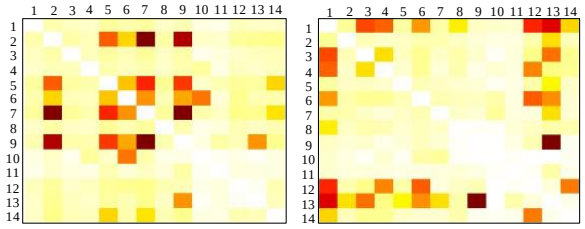

Figure 14. Correlation between different noise categories

Specifically, for a 311 complaint record ns (of the ith category), we count the complaints of other categories φ_j ($1 \le j \le M, j \ne i$) within a circle distance δ to ns, as illustrated in Figure 13. Then the correlation between two categories c_i and c_j can be calculated by Equation 3.

$$Cor(c_i, c_j) = \frac{\sum_{ns \in \Psi, ns.c = c_i} |\varphi_j|}{|c_i| \cdot |c_j|}; \quad c_i \ne c_j;$$

$$\varphi_j = \{ns' | dist(ns.l, ns'.l) \le \delta \wedge ns'.c = c_j\}; \qquad (3)$$

Where $|c_i|$ and $|c_j|$ denote the number of complaints in category c_i and c_j respectively; $\mathbf{\Psi}$ is the collection of 311 data**.** By putting together $Cor(c_i, c_j)$, we formulate matrix $Z \in \mathbb{R}^{M \times M}$. Though tensor $\mathcal{A}$ can capture the correlation between different noise categories to some extent, matrix Z can further intensify the correlation.

Context-Aware Tensor Decomposition

To achieve a higher accuracy of filling in the missing entries of $\mathcal{A}$, we decompose $\mathcal{A}$ with feature matrices X, Y, and Z collaboratively, as illustrated in Figure 15. Matrix X can be factorized into the multiplication of two matrices, $X = R \times U$, where $R \in \mathbb{R}^{N \times d_R}$ and $U \in \mathbb{R}^{d_R \times P}$ are low rank latent factors for regions and geographical features, respectively. Likewise, matrix Y can be factorized into the multiplication of two matrices, $Y = T \times R^T$, where $T \in \mathbb{R}^{L \times d_T}$ is a low rank latent factor matrices for time slots. d_T and d_R are usually very small (in our model $d_T = d_R$);

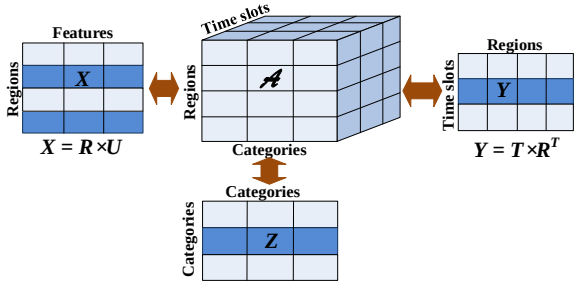

Figure 15. Context-aware tensor decomposition

The objective function is defined as Equation 4:

$$\mathcal{L}(S, R, C, T, U) = \frac{1}{2}\|\mathcal{A} - S \times_R R \times_C C \times_T T\|^2 + \frac{\lambda_1}{2}\|X - RU\|^2 + \frac{\lambda_2}{2}\mathrm{tr}(C^T L_Z C) + \frac{\lambda_3}{2}\|Y - TR^T\|^2 + \frac{\lambda_4}{2}(\|S\|^2 + \|R\|^2 + \|C\|^2 + \|T\|^2 + \|U\|^2) \qquad (4)$$

Where $\|\mathcal{A} - S \times_R R \times_C C \times_T T\|^2$ is to control the error of decomposing $\mathcal{A}$; $\|X - RU\|^2$ is to control the error of factorization of X; $\|Y - TR^T\|^2$ is to control the error of factorization of Y; $\|S\|^2 + \|R\|^2 + \|C\|^2 + \|T\|^2 + \|U\|^2$ is a regularization penalty to avoid over-fitting; $\lambda_1, \lambda_2, \lambda_3$, and λ_4 are parameters controlling the contribution of each part during the collaborative decomposition. When λ_1=λ_2= λ_3= λ_4 =0, our model degenerates to the original tucker decomposition. $C \in \mathbb{R}^{M \times d_C}$, $tr(\cdot)$ denotes the matrix trace; $D_{ii} = \sum_i Z_{ij}$ is a diagonal matrix, and $L_Z = D - Z$ is the Laplacian matrix of the category correlation graph. $tr(C^T L_Z C)$ is obtained through the following deduction, which guarantees two (e.g. the ith and jth) noise categories with a higher similarity (i.e., Z_{ij} is big) should also have a closer distance between the vectors (c_i and c_j) they correspond to in C.

$$\frac{1}{2}\sum_{i,j}\|c_i - c_j\|_2 Z_{ij} = \sum_{i,j} c_i Z_{ij} c_i^T - \sum_{i,j} c_i Z_{ij} c_j^T$$
$$= \sum_{i,j} c_i D_{ii} c_i^T - \sum_{i,j} c_i Z_{ij} c_j^T$$
$$= tr(C^T(D - Z)C) = tr(C^T L_Z C), \qquad (5)$$

where $C^T = \{c_1, c_2, \ldots, c_M\}$.

Finally, we can recover $\mathcal{A}$ by $\mathcal{A}_{rec} = S \times_R R \times_C C \times_T T$.

In our model, $\mathcal{A}$ and X share matrix R; $\mathcal{A}$ and Y share matrix R and T; L_Z influences factor matrix C. The dense representation of X, Y and Z contributes to the generation of a relatively accurate R, C, and T, which reduce the decomposition error of $\mathcal{A}$ in turn. In other words, the knowledge from geographical features, human mobility features, and the correlation between noise categories is propagated into tensor $\mathcal{A}$.

Algorithm 1: Context-Aware Tensor Decomposition

Input: tensor $\mathcal{A}$, matrix X, matrix Y, matrix Z, an error threshold ε
Output: R, C, T, S

1. Initialize $S \in \mathbb{R}^{d_R \times d_U \times d_T}$, $R \in \mathbb{R}^{N \times d_R}$, $C \in \mathbb{R}^{M \times d_C}$, $T \in \mathbb{R}^{2L \times d_T}$, $U \in \mathbb{R}^{d_R \times P}$ with small random values
2. Set η as step size
3. $D_{ii} = \sum_i Z_{ij}$
4. $L_Z = D - Z$
5. **While** $Loss_t - Loss_{t+1} > \varepsilon$
6. **Foreach** $\mathcal{A}_{ijk} \neq 0$
7. $Y_{ijk} = S \times_R R_{i*} \times_C C_{j*} \times_T T_{k*}$;
8. $R_{i*} \leftarrow R_{i*} - \eta\lambda_4 R_{i*} - \eta(Y_{ijk} - \mathcal{A}_{ijk}) \times S \times_C C_{j*} \times_T T_{k*} - \eta\lambda_1(R_{i*} \times U - X_{i*}) \times U - \eta\lambda_3(T \times R_{i*}^T - Y_{*i}) \times T$;
9. $C_{j*} \leftarrow C_{j*} - \eta\lambda_4 C_{j*} - \eta(Y_{ijk} - \mathcal{A}_{ijk}) \times S \times_R R_{i*} \times_T T_{k*} - \eta\lambda_2(L_Z * C)_{j*}$;
10. $T_{k*} \leftarrow T_{k*} - \eta\lambda_4 T_{k*} - \eta(Y_{ijk} - \mathcal{A}_{ijk}) \times S \times_R R_{i*} \times_U C_{j*} - \eta\lambda_3(T_{k*} \times R^T - Y_{k*}) \times R$;
11. $S \leftarrow S - \eta\lambda_4 S - \eta(Y_{ijk} - \mathcal{A}_{ijk}) \times R_{i*} \otimes C_{j*} \otimes T_{k*}$;
12. $U \leftarrow U - \eta\lambda_4 U - \eta\lambda_1(R_{i*} \times U - X_{i*}) \times R_{i*}$;
13. **Return** R, C, U, T, S

Figure 16. Algorithm for the tensor decomposition

Figure 16 presents the algorithm for the collaborative tensor decomposition. As there is no closed-form solution for

finding the global optimal result of the objective function (shown in Equation 3), we use a numeric method, gradient descent, to find a local optimization. Specifically, we use an element-wise optimization algorithm [6], which updates each entry in the tensor independently.

EVALUATION

Datasets

Table 2 summarizes the information of the four data sets; Table 3 further details the road network data. Road segments with a level from L_1 to L_5 are used to partition NYC, resulting in 891 regions. As weekdays and weekends have different noise situations, we build an individual tensor for them. If setting 1 hour as a time slot, the size of the two tensors is 891×14×24. The time length of a time slot can be adjusted based on applications. By feeding the 311 data of 168 weekdays and 68 weekends into the two tensors, we obtain 7.39% non-zero entries (i.e., the entry's value≥1) on weekdays and 5.18% on weekends, as shown in Table 4. However, one complaint in an hour may not be safe enough, which could be a false record. Setting a higher threshold to determine a none-zero entry improves the quality of an individual entry's value, but leading to a worse data sparsity. Considering the trade-off, we set threshold=2 here. Thus, 291,143 cells in the weekday tensor and 293,897 cells in the weekend tensor need supplemented by the inference.

Table 2. Description on datasets

Data sets	Period	Scales
311 noise data	5/23/2013-1/31/2014	67,378; 14 categories
Foursquare	4/24/2009-10/13/2013	173,275
Gowalla	5/5/2008-7/23/2011	127,558
POIs	2013	26,884; 15 categories
Road Network	2013	87,898 nodes, 91,649 edges

Table 3. Statistics on NYC's road network data

Lev	Num. edges	Length	Lev	Num. edges	Length
L_1	3,236	381	L_4	8,409	699
L_2	4,816	677	L_5	1,906	1,321
L_3	762	54	L_6	96,934	9,279
		KM	Total	133,225	12,412

Table 4. The sparseness of the tensor with different thresholds

Data sets	Threshold=1	Threshold=2	Threshold=3
Weekdays	7.39%	2.75%	1.49%
Weekends	5.18%	1.83%	1.01%

Evaluation on the Tensor Model

We evaluate the context-aware tensor decomposition model in two approaches. In the first approach, we randomly remove 30% non-zero entries from the tensor and fill in these entries using our model. We then use the original values of these entries as a ground truth to measure the inferred values. In the second approach, we perform an in-the-field study in 36 locations in Manhattan (24 in the daytime and 12 in the nighttime), collecting the real noise level of each location via a mobile phone's microphone. We then rank these locations in terms of the real noise level and the inferred values respectively, measuring the closeness of the two ranks using NDCG (Normalized Discounted cumulative gain) [22].

Table 5 shows the results of the first evaluation approach, in which we compare our model with four baselines: 1) *AWR* fills a missing entry with the average of all non-zero entries that pertain to the region; 2) *AWH* fills in a missing entry with the average of all entries belonging to the time slot; 3) *MF* fills the missing entries by factorizing the region-category matrix hour by hour; 4) *Kriging* interpolates the noise of a missing entry with the non-zero entries geospatially nearby. We also study the contribution of matrix X, Y, and Z in helping supplement the missing entries. The performance is measured by two metrics: Root Mean Square Error (RMSE) and Mean Absolute Error (MAE), where $\hat{y}_i$is an inference and y_i is the ground truth; n is the number of instances.

$$RMSE = \sqrt{\frac{\sum_i (y_i - \hat{y}_i)^2}{n}}, \quad (6)$$

$$MAE = \frac{\sum_i |y_i - \hat{y}_i|}{n}, \quad (7)$$

Table 5. Performance comparison of different methods

Methods	Weekdays		Weekends	
	RMSE	MAE	RMSE	MAE
AWR	4.736	2.582	4.446	2.599
AWH	4.631	2.461	4.42	2.522
MF	4.600	2.474	4.393	2.516
Kriging	4.59	2.424	4.253	2.495
TD	4.391	2.381	4.141	2.393
TD+ X	4.285	2.279	4.155	2.326
TD+ X + Y	4.160	2.110	4.003	2.198
TD+ X + Y+ Z	**4.010**	**2.013**	**3.930**	**2.072**

Figure 17 presents the performance of the second evaluation approach, where our method outperforms the method only using 311 noise complaints. The higher NDCG is the better ranking performance is. The results validate the capability of our model in differentiating between locations with different noise levels in the same time span [12].

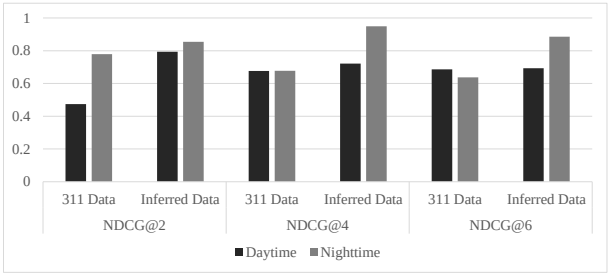

Figure 17. Performance of in-the field study

Results

Figure 18 presents six heat maps of NYC in different time spans of weekdays and weekends, in terms of the overall noise pollution indicator of a region, i.e., $\sum_j \sum_k \mathcal{A}_{rec}(i,j,k)$. As mentioned previously, the noise pollution indicator is a result of two factors: the noise level in a location and people's reaction (or tolerance) to the noises. So, we can understand the heat maps in the following way: to what extent people would feel uncomfortable due to the noises in a given time span and a region. The deeper the color is, the higher the probability of feeling uncomfortable. Generally,

people complain more about noise pollution on weekends as 1) they have time to complain and 2) their tolerance to noise is lower than on weekdays. Particularly, during the night (0-5am) when people expect to have quality sleep, their tolerance to noise pollution is very low; so, the noise pollution indicator is higher than other time slots, as shown in the bottom-left part of Figure 18. More specifically, the region where Columbia University is located has a heavier noise pollution than other areas, while Central Park is generally a quieter place.

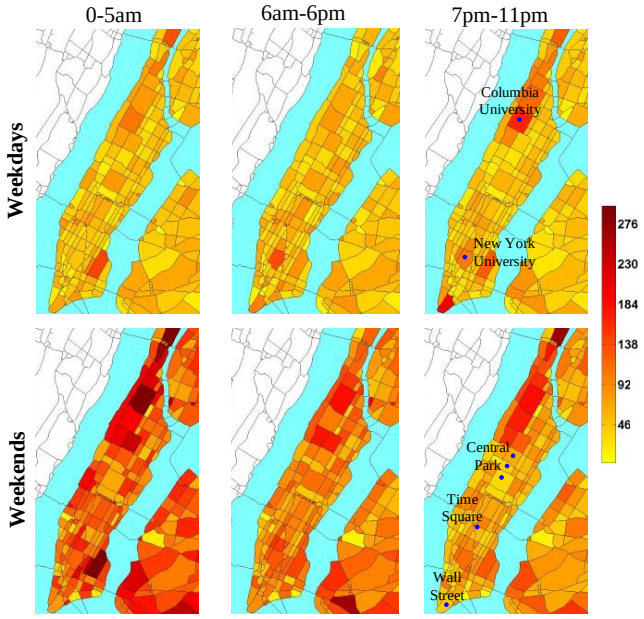

Figure 18. Overall noise situation in NYC

Figure 19 shows the noise composition of the five locations marked in Figure 18. The noise indicators of the five regions is a summation of their own individual noise indicators in each hour and on both weekends and weekdays. Columbia University and Wall Street have a heavier noise situation than other places. The largest noise category in Wall Street is *Construction* while the other four is *Loud music/Party*.

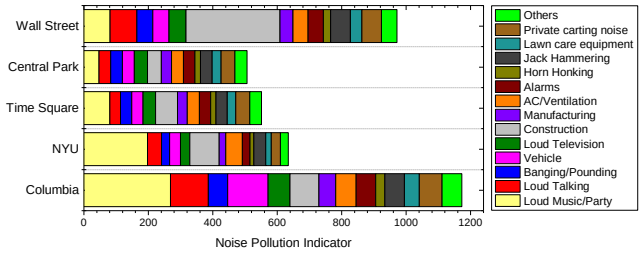

Figure 19. Noise composition of five well-known places in NYC

Figure 20 further compares the noise pollution indicator of the top six noise categories, changing over time of day, at Columbia University and New York University (NYU), where we find some similarities and differences. Both locations have two spikes in the daytime; the same one is at 6am. But, the second spike of NYU comes earlier than Columbia. The noise pollution caused by *Loud Music* reaches a local peak at 12pm, indicating that the party time starts earlier at NYU than Columbia University. Additionally, *Air condition/ventilation* and *Jack Hamming* in NYU have a higher presence than Columbia University. It is quite true that quite a few regions around NYU are under construction.

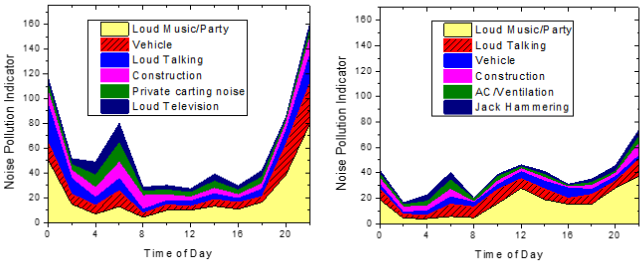

A) Columbia University B) New York University

Figure 20. Top six noise categories changing over time

Figure 21 presents the heat maps of NYC in terms of the noise pollution indicator in four different categories, from 7pm-11pm. Weekends generally have a heavier noise pollution of *Loud music*, while weekdays have more *Construction* noise pollution. Specifically, the strip region marked in the first column is Riverbank State Park, where many people entertain themselves with loud music on weekends. On the contrary, as illustrated in the second column, the region where Columbia University is located has less *Loud talking* noise pollution on weekends, as many students may be off the campus. Yankee Stadium, marked in the third column, has a heavier vehicle noise on weekends, because many people drive there to watch baseball games.

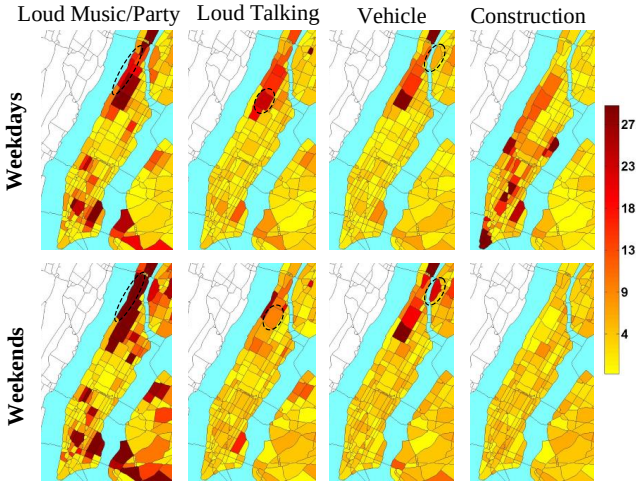

Figure 21. Noise situation of specific categories in NYC.

Figure 22 compares the heat maps built based on 311 data and our inference values, illustrating the value of our model. Without recovering the noises of missing locations, we can barely see vehicle noises from 6am-6pm on weekends. After the inference, we find that the regions close to bridges (marked by the dotted circles) are suffering from vehicle noises. According to our experiences visiting these places, the vehicles passing by the bridges are quite noisy. Likewise, without using our model, we cannot find loud talking to be a problem at Times Square and Columbia University either.

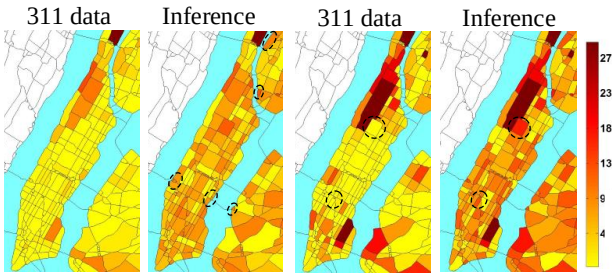

A) Vehicles (6am-6pm) B) Loud Talking (0-5am)

Figure 22. Comparison of heat maps in weekend

RELATED WORK

Urban Noise Sensing

The first step towards understanding noise pollution is to monitor noises. Silvia et al. [4][17][18] propose using wireless sensor networks to monitor environmental noise pollution in urban areas. To deploy and maintain a citywide sensor network, especially in major cities like NYC, however, is very expensive, in terms of money and human resources. Another solution is to leverage crowdsourcing, where people collect and share their ambient environmental information using a mobile device, e.g., a smart phone [10][15][20]. For example, NoiseTube [8] presents a person-centric approach that leverages noise measurements shared by mobile phone users to paint a noise map in a city [3][19]. Because we cannot guarantee having a user reporting their ambient noises anywhere and anytime, the noise map generated through this approach is usually very sparse. As mentioned before, urban noises change by location and over time non-linearly; Thus, we cannot use a linear interpolation to fill the missing places in the map. To deal with this issue, Rajib et al. [16] proposed to recover a noise map from incomplete and random samples based on compressive sensing.

Though our method is also a crowd sensing-based approach, the differences between our research and the above-mentioned works lie in three aspects. First, beyond raw sensor data, the 311 data we use does not indicate the noise levels but also people's reaction and tolerance to noise. Second, besides recovering the noise pollution of a city, our method also explores the distribution of noises over different categories. The information can inform governmental authorities' decision making on tackling noise pollution. Third, when dealing with the data sparsity problem, we incorporate other data sources, such as user check-ins and POIs. According to the experimental results and data analytics, these datasets have a correlation with urban noises, therefore helping supplement the noise situation of places without sufficient 311 data.

Noise Understanding

A number of works [2][5][9][11][13] have focused on classifying environmental noises so as to understand a user's contexts, such as in a car or on a street. For example, Couvreur and Bresleer [2] propose a statistical framework for a noise event recognition, including noises from cars, trucks and airplanes. This approach works for recognizing a separated noise event rather than mixed noise sources [9]. Later, Gainard et al. [5] proposed a hidden Markov model (HMM)-based classifier to recognize five noise events (car, truck, moped, aircraft and train), which is claimed to be better than human listeners. Ma et al. [9] use a HMM-based strategy capable of classifying ten environments. SoundSense [13] combines supervised and unsupervised learning techniques to classify not only general sound types (e.g., music) but also novel sound events.

Our method differs from the above-mentioned approaches in two aspects. First, diagnosing the composition of noises in a location is different from classifying the environmental contexts of a user. The output of the latter is usually a probability distribution over possible noise categories, where the category with the biggest probability is used as a prediction. In our method, instead, the proportion of 311 complaints of different noise categories in a location could well describe the composition of the noises in the location. Second, applying such classification methods to a major city like NYC needs a huge volume of training data that covers different locations and time spans. However, we model urban noises with a 3D tensor, which incorporates the temporal correlation among different time slots and the spatial correlation among different locations to recover a location's noises. Using a tensor decomposition-based method, which is an unsupervised approach, we can obtain the composition of noises in a location based on sparse data.

Tensor Decomposition for Urban Computing

The method of tensor decomposition incorporating multiple datasets has been widely used in urban computing [30]. [21][23][28][29] used a context-aware tensor decomposition incorporating additional information, such as the activity-activity correlation and geographical features of a location, to conduct different kinds of recommendations. Tensor factorization was also applied in [27] to infer urban refueling behavior, together with POI data, traffic features, and gas stations' contextual features. Sharing the similar approach with these works, our goal is different from theirs and more data sources (e.g., user check-ins) are included.

CONCLUSION

In this paper, we diagnose the noise pollution in NYC using four data sources: 311 complaint data, social media, POIs and road network data. We model the noise in NYC with a three dimension tensor, filling in the missing entries of the tensor using a context-aware tensor decomposition approach. A noise pollution indicator is generated for each region in a time span and a noise category. The indicator reflects not only the level of noise in a location but also people's tolerance to noise during different time spans. This is an approach of using human as a sensor and crowd sensing implicitly. With the research, we can rank locations by using the noise pollution indicator (individually or aggregately) and study the composition of noises in arbitrary locations. We evaluate our model with extensive experiments and validate its advantages beyond four baseline methods. The data we use in the research has been released at [31], and a demonstration is available at [32].

REFERENCES

1. 311. http://nycopendata.socrata.com/Social-Services/311-Service-Requests-from-2010-to-Present/erm2-nwe9
2. Couvreur, C. Environmental sound recognition: a statistical approach. Facult'e Polytechnique de Mons, Phd Thesis, 1997.
3. D'Hondt, E., and Stevens, M. Participatory noise mapping. In Demo Proceedings of the 9th International Conference on Pervasive Computing, pp. 33–36.
4. Filipponi, L., Santini, S., and Vitaletti, A. Data collection in wireless sensor networks for noise pollution monitoring. In *Proc. DCOSS 2008*, IEEE Press (2008), 492-497.
5. Gaunard, P., Mubikangiey, C. G., Couvreur, C., and Fontaine, V. Automatic classification of environmental noise events by hidden Markov models. Applied Acoustics, 1998.
6. Karatzoglou, A., Amatriain, X., Baltrunas, L., and Oliver, N. Multiverse recommendation: n-dimensional tensor factorization for context-aware collaborative filtering. In *Proc. RecSys 2010*, ACM Press (2010), 79-86.
7. Kolda, T. G., and Bader, B. W. Tensor decompositions and applications. SIAM review, 51, 3(2009): 455-500.
8. Maisonneuve, N., Stevens, M., Niessen, M. E., and Steels, L. NoiseTube: Measuring and mapping noise pollution with mobile phones. In *Proc. ITEE 2009*, Springer Berlin Heidelberg, 215-228.
9. Ma, L., Smith, D., and Milner, B. Environmental noise classification for context-aware applications. In *Proc. DEXA 2003*, Springer Berlin Heidelberg, 360-370.
10. Lane, N. D., Miluzzo, E., Lu, H., Peebles, D., Choudhury, T., and Campbell, A. T. A survey of mobile phone sensing. Journal of Communications Magazine, IEEE, 48, 9(2010): 140-150.
11. Li, D., Sethi, I. K., Dimitrova, N., and McGee, T. Classification of general audio data for content-based retrieval. Journal of Pattern recognition letters, 22, 5 (2001): 533-544.
12. Liu, T., Zheng, Y., Liu, L., Liu, Y., Zhu, Y. Methods for sensing urban noises. MSR-TR-2014-66, May 2014.
13. Lu, H., Pan, W., Lane, N. D., Choudhury, T., and Campbell, A. T. SoundSense: scalable sound sensing for people-centric applications on mobile phones. In *Proc. MobiSys 2009*, ACM Press (2009), 165-178.
14. Oliver, Margaret A., and R. Webster. Kriging: a method of interpolation for geographical information systems. Journal of Geographical Information System, 4, 3(1990): 313-332.
15. Pushp, S., Min, C., Lee, Y., Liu, C. H., and Song, J. Towards crowd-aware sensing platform for metropolitan environments. In *Proc. SenSys 2012*, ACM Press (2012), 335-336.
16. Rana, R. K., Chou, C. T., Kanhere, S. S., Bulusu, N., and Hu, W. Ear-phone: an end-to-end participatory urban noise mapping system. In *Proc. IPSN 2010*, ACM Press (2010), 105-116.
17. Santini, S., Ostermaier, B., and Vitaletti, A. First experiences using wireless sensor networks for noise pollution monitoring. In *Woekshop on REALWSN 2008*, ACM Press (2008), 61-65.
18. Santini, S., and Vitaletti, A. Wireless sensor networks for environmental noise monitoring. 6. Fachgespr ̈ch Sensornetzwerke (2007), 98.
19. Stevens, M., and D'Hondt, E. Crowdsourcing of pollution data using smartphones. In *Workshop on Ubiquitous Crowdsourcing 2010*.
20. Xu, C., Li, S., Liu, G., Zhang, Y., Miluzzo, E., Chen, Y. F., Li, J., and Firner, B. Crowd++: unsupervised speaker count with smartphones. In *Proc. Ubicomp 2013*, ACM Press (2013), 43-52.
21. Yang, D., Zhang, D., Yu, Z., and Yu, Z. Fine-grained preference-aware location search leveraging crowdsourced digital footprints from LBSNs. In *Proc. Ubicomp 2013*, ACM Press (2013), 479-488.
22. Yilmaz, E., Kanoulas, E., and Aslam, J. A. (2008, July). A simple and efficient sampling method for estimating AP and NDCG. In *Proc. SIGIR 2008*, ACM Press (2008), 603-610.
23. Wang, Y., Zheng, Y., Xue, Y. Travel Time Estimation of a Path using Sparse Trajectories. In *Proc. of KDD 2014*.
24. Yuan, N. J., Zheng, Y., and Xie, X. Segmentation of urban areas using road networks. MSR-TR-2012-65. 2012.
25. Yuan, N. J., Zheng, Y., and Xie, X. Discovering regions of different functions in a city using human mobility and POIs. In *Proc. KDD 2012*, ACM Press (2012), 186-194.
26. Zhang, A. X., Noulas, A., Scellato, S., and Mascolo, C. Hoodsquare: Modeling and Recommending Neighborhoods in Location-based Social Networks. In *Proc. SocialCom 2013*, IEEE Press (2013), 69-74.
27. Zhang, F., Wilkie, D., Zheng, Y., and Xie, X. Sensing the pulse of urban refueling behavior. In *Proc. UbiComp 2013*, ACM Press (2013), 13-22.
28. Zheng, V. W., Cao, B., Zheng, Y., Xie, X., and Yang, Q. Collaborative Filtering Meets Mobile Recommendation: A User-centered Approach. In *Proc. AAAI 201*0, ACM Press (2010), 236-241.
29. Zheng, V. W., Zheng, Y., Xie, X., and Yang, Q. Towards mobile intelligence: Learning from GPS history data for collaborative recommendation. Journal of Artificial Intelligence, 184(2012): 17-37.
30. Zheng, Y., Capra, L., Wolfson, O., Yang, H. Urban Computing: concepts, methodologies, and applications. ACM Trans. on Intelligent Systems and Technology, 5, 3 (2014).
31. Data and executable files released at: http://research.microsoft.com/apps/pubs/?id=217236
32. Wang, Y., Zheng, Y., Liu, T. A noise map of New York City. In Proc. of UbiComp 2014. Demo Paper.